IUCrData

ISSN 2414-3146

2-Azido-*N*-(*o*-tolyl)acetamide

Abderrazzak El Moutaouakil Ala Allah,[a] Musa A. Said,[b] Vera Lederer,[c] Biprajit Sarkar,[c] Abdulsalam Alsubari,[d]* Joel T. Mague[e] and Youssef Ramli[a]*

[a]Laboratory of Medicinal Chemistry, Drug Sciences Research Center, Faculty of Medicine and Pharmacy, Mohammed V University in Rabat, Morocco, [b]Department of Chemistry, Faculty of Science, Islamic University of Madinah, Madinah, 42351, Saudi Arabia, [c]Institut fur Chemie und Biochemie, Anorganische Chemie, Freie Universität Berlin, Fabeckstrasse 34-36, 14195 Berlin, Germany, [d]Laboratory of Medicinal Chemistry, Faculty of Clinical Pharmacy, 21 September University for Medical and Applied Sciences, Yemen, and [e]Department of Chemistry, Tulane University, New Orleans, LA 70118, USA. *Correspondence e-mail: alsubarinag@21umas.edu.ye, y.ramli@um5r.ac.ma

Received 7 October 2026
Accepted 12 October 2026

Edited by L. Van Meervelt, Katholieke Universiteit Leuven, Belgium

Keywords: crystal structure; azide; hydrogen bond; acetamide; C—H···π(ring) interaction; Hirshfeld surface.

CCDC reference: 2594679

Structural data: full structural data are available from iucrdata.iucr.org

In the title molecule, $C_9H_9N_3O$, the inner C—N—C—C portion is almost planar and the phenyl ring and azide group are rotated to be well out of this plane. In the crystal, N—H···O and C—H···O hydrogen bonds plus C—H···π(ring) interactions form chains of molecules extending along the *a*-axis direction, which pack with normal van der Waals interactions.

3D view

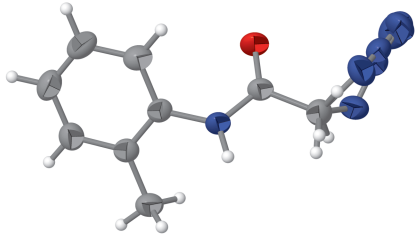

Chemical scheme

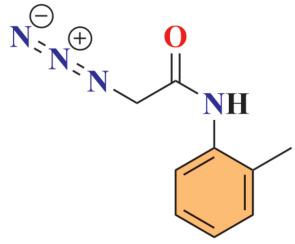

Structure description

A main target in medicinal chemistry is heo synthesis of compounds or libraries of compounds through a variety of chemical reactions during the drug discovery process (Patrick, 2023). Among the numerous synthetic methodologies available, the 1,3-dipolar cycloaddition, also known as the Huisgen cycloaddition, is widely employed for the construction of bioactive molecules (Huisgen *et al.*, 1967). This reaction involves the cycloaddition of an organic azide with a terminal alkyne, leading to the formation of 1,4- or 1,5-disubstituted 1,2,3-triazoles, depending on the catalyst and reaction conditions employed (Johansson *et al.*, 2016). Alkyl azides are regarded as key synthetic intermediates in medicinal chemistry because they provide efficient access to 1,2,3-triazole derivatives, a privileged heterocyclic scaffold that has been extensively exploited in the development of therapeutic agents for the treatment of a wide range of diseases (Zhou & Wang, 2012). With this objective in mind, and as a continuation of our ongoing research (*e.g.* Guerrab *et al.*, 2025), we report herein the synthesis and structural characterization of the title compound, $C_9H_9N_3O$ (**2**), prepared *via* nucleophilic substitution of the corresponding *N*-aryl chloroacetamide precursor with sodium azide. The molecular structure of **2** is shown in Fig. 1.

OPEN ACCESS
Published under a CC BY 4.0 licence

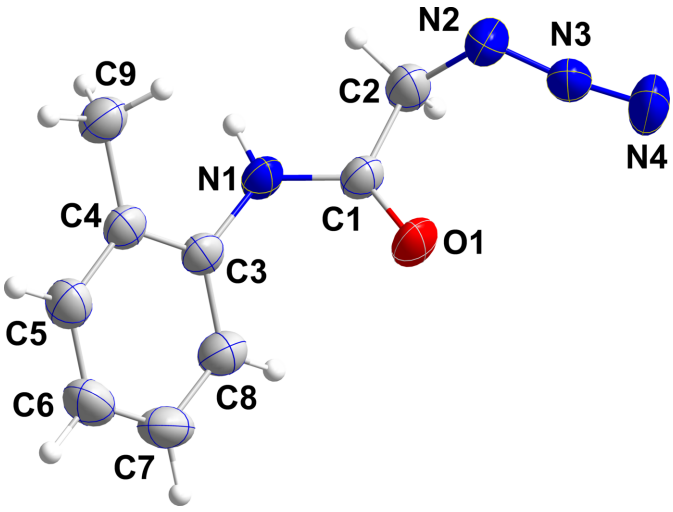

Figure 1
Perspective view of the title molecule with labeling scheme and 50% probability ellipsoids. Only the major orientation of the azide group is shown.

The C3—N1—C1—C2 portion is planar within experimental error [torsion angle C3—N1—C1—C2 is −179.52 (14)°]. Both the azide and phenyl moieties are rotated out of this plane as indicated by the C1—N1—C3—C4 torsion angle of 131.37 (16)° and the dihedral angle between the amide group (O1/C1/N1) and benzene ring (C3–C8) of 48.4 (2)°. Bond lengths and interbond angles are as expected for the formulation given.

In the crystal, N1—H1···O1^{i} and C2—H2AB···O1^{i} hydrogen bonds plus C9—H9*C*···*Cg*1^{i} interactions (*Cg*1 is the centroid of the C3–C8 ring; Table 1) form chains of molecules extending along the *a*-axis direction (Fig. 2). The chains pack with normal van der Waals interactions.

A search of the Cambridge Structural Database (CSD, version 6.01, updated to June 2026; Groom *et al.*, 2016) with the fragment shown in Fig. 3 (*R* = C) yielded 85 hits. Many of these contained the N_3 fragment as part of a triazole or a

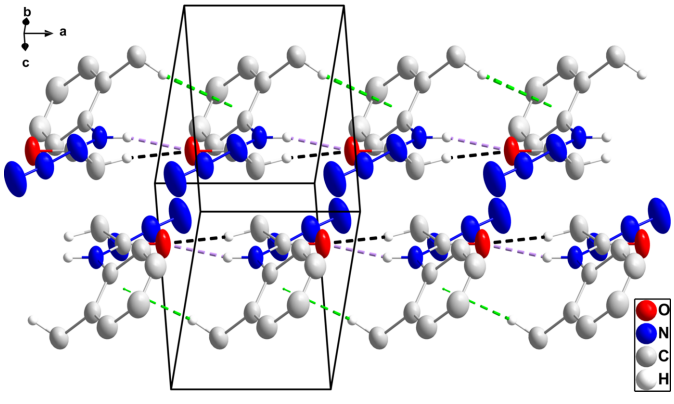

Figure 2
Packing projected onto (011) with N —H···O and C—H···O hydrogen bonds depicted, respectively, by violet and black dashed lines. The C—H···π(ring) interactions are depicted by green dashed lines and non-interacting hydrogen atoms are omitted for clarity.

Table 1
Hydrogen-bond geometry (Å, °).

*Cg*1 is the centroid of the C3–C8 benzene ring.

D—H···*A*	*D*—H	H···*A*	*D*···*A*	*D*—H···*A*
N1—H1···O1^{i}	0.87 (2)	2.14 (2)	2.9918 (15)	166 (2)
C2—H2*AB*···O1^{i}	0.98	2.37	3.2576 (19)	150
C9—H9*C*···*Cg*1^{i}	0.97	2.81	3.5817 (18)	137

Symmetry code: (i) $x+1, y, z$.

tetrazole ring, which left 20 that are comparable to the title molecule. These are listed in Table 2 with the more complex *R* groups pictured in Fig. 4. Inspection of the torsion angles corresponding to the N1—C1—C2—N2 and C1—N1—C3—C4 torsion angles in the title molecule (Table 2) shows that in the similar molecules, the conformations vary widely. Since the *R* groups vary greatly in size and shape, this is not surprising and likely can be attributed to packing considerations.

The d_{norm} Hirshfeld surface of the title molecule was calculated with *CrystalExplorer* (Spackman *et al.*, 2021) and is shown in Fig. 5. Descriptions of the plots obtained by this method and their interpretations have been published (Tan *et al.*, 2019). In Fig. 5, the intense red spots indicate the locations of the N—H···O hydrogen bonds to the neighboring molecules while the C—H···O hydrogen bonds are indicated by lighter red spots and the C—H···π(ring) interaction by the green line. The two-dimensional fingerprint plots are shown in Fig. 6 with all interactions in Fig. 6*a*, and the H···H interactions in Fig. 6*b*. The latter contribute 32.6% of the total intermolecular contacts which is often the case for organic molecules whose periphery consists largely of hydrogen atoms. It might be surprising that the N···H/H···N contacts (Fig. 6*c*)

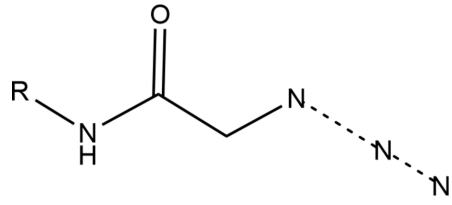

Figure 3
The search fragment used for the CSD database survey (*R* = C).

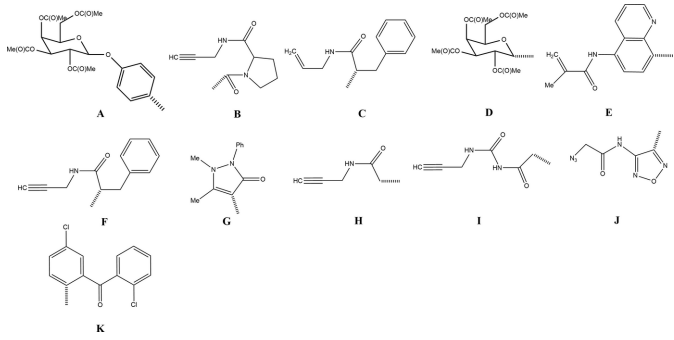

Figure 4
The substituents (*R*) referred to in Table 2. The wide dashed bond indicates the point of attachment.

Table 2
Results of CSD database survey.

Compound	R^a	Torsion 1^b (°)	Torsion 2^c (°)	Reference
Title molecule	*o*-tolyl	132.74 (16)	131.37 (16)	This work
ASEDIO	phenyl	169.90 (18), 160.9 (2)	151,3(3), 161.5 (2)	Guerrab *et al.* (2021)
BEBPIJ	A	−17.4 (13)	−164.4 (10)	Cecioni *et al.* (2012)
BEKRES	*p*-tolyl	−177.75 (18), −176.64 (18), −179.23 (18)	−156.8 (2), −160.2 (2), −158.8 (2)	Missioui *et al.* (2022*a*)
BEKRIW	4-FC_6H_4	167.98 (18), −156.64 (18)	−158.4 (2), −158.8 (2)	Missioui *et al.* (2022*b*)
CUVVEY	2,6-$Me_2C_6H_3$	−137.3 (5), 136.6((4)	−116.5 (6), 114.9 (5)	El Moutaouakil Ala Allah *et al.* (2025)
DAPYOU	4-$HC_2C_6H_4$	−160.0 (4), −175.4 (3)	−176.2 (4), 168.4 (3)	Madhusudhanan *et al.* (2021)
GUYCUC	B	103.7 (9)	−78.2 (6)	Rai *et al.* (2025)
HIQKIF	C	−145.6 (4)	−126.0 (3)	Khazeber & Sureshan (2022)
KEPKOG	D	6.5 (2)	126.8 (4)	Petsalakis *et al.* (2006)
LETTIR	E	5.7 (3)	1.6 (4)	Guirado-Moreno *et al.* (2023)
PADGEK	F	166.5 (7)	118.6 (6)	Hema & Sureshan (2020)
QAGNOF	4-$O_2NC_6H_4$	142.68 (13)	15.99 (19)	Missioui *et al.* (2020)
QIMYOE	G	123.53 (9)	68.76 (12)	Kumar *et al.* (2023)
TARHIH	4-$MeOC_6H_4$	125.25 (14)	156.34 (15)	Missioui *et al.* (2022*c*)
TODFIZ	H	−161.8 (8)	−173.9 (8)	Athiyarath & Sureshan (2019)
TODVAM	I	161.9 (4)	178.0 (4)	Athiyarath & Sureshan (2019)
TUZPEJ	J	10.0 (3), 176.0 (2)	146.9 (3), 37.3 (4)	Li *et al.* (2003)
VIFVOX	K	−170.3 (3), −3.8 (4)	161.9 (2), 174.7 (2)	Sandra *et al.* (2012)
WOQBOX	$PhCH_2CH_2$	177.98 (13)	84.67 (17)	Cedillo-Cruz *et al.* (2024)

Notes: (*a*) Letters refer to the drawings in Fig. 4; (*b*) corresponds to the N1—C1—C2—N2 torsion in the title molecule; (*c*) corresponds to the C1—N1—C3—C4 torsion in the title molecule.

comprise 33.3% of the total since there are no directed hydrogen bonds to nitrogen. However, with the considerable nitrogen content due to the azide group, there are six N···H contacts at or close to the sum of the respective van der Waals radii. The other significant contributions come from the C···H/H···C (Fig. 6*d*, 17.3%) and the O···H/H···O (Fig. 6*e*, 10.5%) contacts. The former are due primarily to the C—H···π(ring) interactions and appear as a pair of rather blunt peaks. The latter appear as a pair of sharp peaks attributed to the N—H···O hydrogen bonds with broader shoulders which correspond to the C—H···O hydrogen bonds.

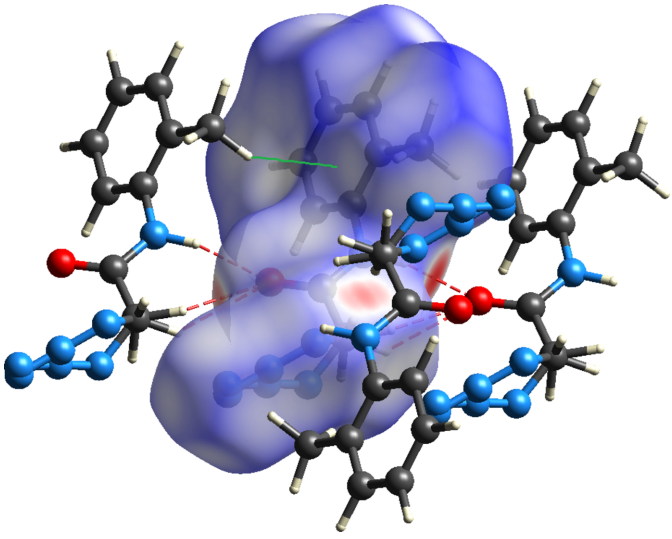

Figure 5
The d_{norm} Hirshfeld surface of the title molecule together with neighboring molecules and indicating the hydrogen bonds (red dashed lines) and C—H···π(ring) interactions (green line).

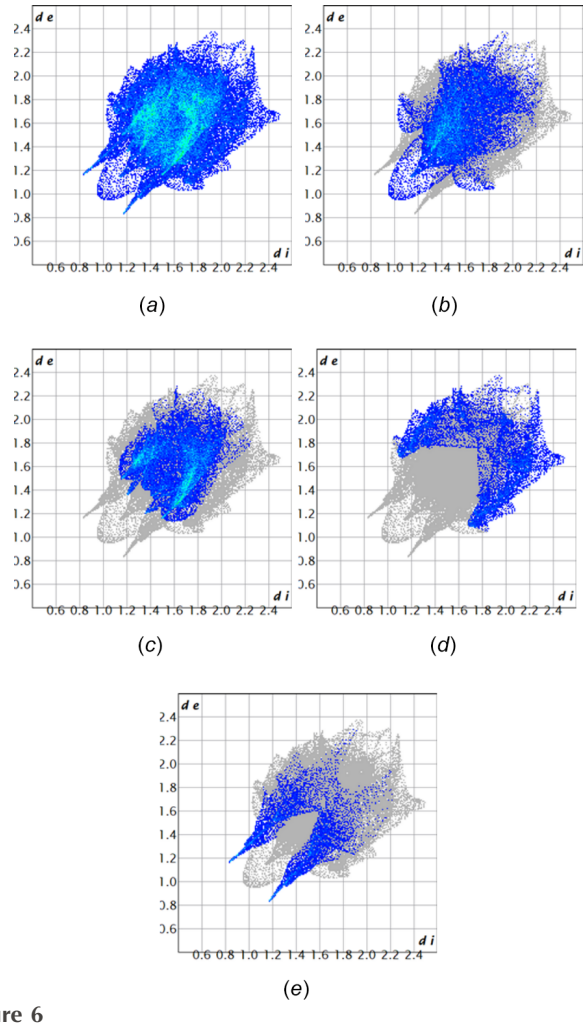

Figure 6
Two-dimensional fingerprint plots showing all intermolecular interactions (*a*), the H···H interactions (*b*), the N···H/H···N interactions (*c*), the C···H/H···C interactions (*d*) and the O···H/H···O interactions (*e*).

Table 3
Experimental details.

Crystal data	
Chemical formula	$C_9H_{10}N_4O$
M_r	190.21
Crystal system, space group	Triclinic, $P\overline{1}$
Temperature (K)	250
a, b, c (Å)	4.8642 (6), 9.9359 (13), 10.4042 (9)
α, β, γ (°)	70.153 (10), 87.279 (8), 84.833 (10)
V (Å^3)	470.97 (10)
Z	2
Radiation type	Cu $K\alpha$
μ (mm^{-1})	0.77
Crystal size (mm)	0.46 × 0.16 × 0.13
Data collection	
Diffractometer	SuperNova, Dual, Cu at home/near, Atlas
Absorption correction	Gaussian (*CrysAlis PRO*; Rigaku OD, 2026)
T_{min}, T_{max}	0.474, 1.000
No. of measured, independent and observed [$I > 2\sigma(I)$] reflections	2964, 1787, 1446
R_{int}	0.018
(sin $\theta/\lambda)_{max}$ (Å^{-1})	0.619
Refinement	
$R[F^2 > 2\sigma(F^2)]$, $wR(F^2)$, S	0.039, 0.116, 1.05
No. of reflections	1787
No. of parameters	159
No. of restraints	48
H-atom treatment	H atoms treated by a mixture of independent and constrained refinement
$\Delta\rho_{max}$, $\Delta\rho_{min}$ (e Å^{-3})	0.22, −0.16

Computer programs: *CrysAlis PRO* (Rigaku OD, 2026), *SHELXT2018/2* (Sheldrick, 2015*a*), *SHELXL2018/3* (Sheldrick, 2015*b*) and *OLEX2* (Dolomanov *et al.*, 2009).

Synthesis and crystallization

The precursor 2-chloro-*N*-(*o*-tolyl)acetamide (**1**) was prepared according to the procedure described in our previous work (*e.g.* El Moutaouakil Ala Allah *et al.*, 2024). A mixture of 2.73 mmol of compound **1** and 3.52 mmol of sodium azide was dissolved in an ethanol/water mixture and refluxed at 80 °C for 24 h. Upon completion of the reaction, as monitored by thin-layer chromatography (TLC), the precipitated 2-azido-*N*-(*o*-tolyl)acetamide (**2**) was collected by filtration and washed with cold water. The resulting solid was subsequently recrystallized from ethanol. Single crystals suitable for X-ray diffraction analysis were obtained by slow evaporation from ethanol solution.

Yield 82%, white solid, m.p. = 455–457 K. FT–IR (ATR, cm^{-1}): 3218 (NH), 2110 (N_3), 1640 (C═O); ^{1}H NMR (500 MHz, DMSO-d_6): δ p.p.m. 4.18 (*s*, 2H, CH_2), 4.32 (*s*, 3H, CH_3), 6.72–7.30 (*m*, 4H, Ar—H), 10.82 (*s*, 1H, NH); ^{13}C NMR: 44.25 (CH_2), 48.23 (CH_3), 118.62, 121.25, 134.62, 148.59 (C—Ar); 169.23 (C═O).

Refinement

Crystal data, data collection and structure refinement details are summarized in Table 3. The azide group is disordered over two sites related by a 22.4 (3)° rotation about the C1—C2 bond in a 0.740 (4)/0.260 (4) ratio. The two components were refined with restraints that their geometries be comparable.

Acknowledgements

YR is thankful to the National Center for Scientific and Technical Research of Morocco (CNRST) for its continuous support. Author contributions are as follows. Conceptualization, YR; methodology, AA and MAS; investigation, AEMA.; writing (review and editing of the manuscript), YR; formal analysis, JTM and VL; supervision, YR; crystal structure determination, BS.

References

Athiyarath, V. & Sureshan, K. M. (2019). *Angew. Chem. Int. Ed.* **58**, 612–617.
Cecioni, S., Praly, J.-P., Matthews, S. E., Wimmerová, M., Imberty, A. & Vidal, S. (2012). *Chem. Eur. J.* **18**, 6250–6263.
Cedillo–Cruz, A., Villalobos–López, D. C., Zavala–Segovia, N., Aguilar, M. I. & Cuevas–Yañez, E. (2024). *J. Mol. Struct.* **1309**, 138178.
Dolomanov, O. V., Bourhis, L. J., Gildea, R. J., Howard, J. A. K. & Puschmann, H. (2009). *J. Appl. Cryst.* **42**, 339–341.
El Moutaouakil Ala Allah, A., Kariuki, B. M., Al-Sulami, A. I., Basha, M. T., Allehyani, B. H., Alsubari, A., Mague, J. T. & Ramli, Y. (2025). *Acta Cryst.* E**81**, 627–631.
El Moutaouakil Ala Allah, A., Kariuki, B. M., Ameziane El Hassani, I., Alsubari, A., Guerrab, W., Said, M. & Ramli, Y. (2024). *IUCrData* **9**, x241015.
Groom, C. R., Bruno, I. J., Lightfoot, M. P. & Ward, S. C. (2016). *Acta Cryst.* B**72**, 171–179.
Guerrab, W., Missioui, M., Zaoui, Y., Mague, J. T. & Ramli, Y. (2021). *Z. Kristallogr. New Cryst. Struct.* **236**, 133–134.
Guerrab, W., Mortada, S., El Moutaouakil Ala Allah, A., Demirtaş, G., Mague, J. T., Alzahrani, A. Y. A., AL Mughram, M. H., Faouzi, M. E. A. & Ramli, Y. (2025). *J. Mol. Struct.* **1333**, 141802.
Guirado-Moreno, J. C., González-Ceballos, L., Carreira-Barral, I., Ibeas, S., Fernández-Muiño, M. A., Teresa Sancho, M., García, J. M. & Vallejos, S. (2023). *Spectrochim. Acta A Mol. Biomol. Spectrosc.* **284**, 121820.
Hema, K. & Sureshan, K. M. (2020). *Angew. Chem. Int. Ed.* **59**, 8854–8859.
Huisgen, R., Szeimies, G. & Möbius, L. (1967). *Chem. Ber.* **100**, 2494–2507.
Johansson, J. R., Beke-Somfai, T., Said Stålsmeden, A. & Kann, N. (2016). *Chem. Rev.* **116**, 14726–14768.
Khazeber, R. & Sureshan, K. M. (2022). *Proc. Natl Acad. Sci. USA* **119**, e2205320119.
Kumar, S., Lal, B., Tittal, R. K., Singh, G., Singh, J., Sharma, R. & Sabane, J. K. (2023). *Sens. Diagn.* **2**, 1267–1276.
Li, Z.-X., Tang, S.-Q., Liu, J.-T. & Sun, J. (2003). *Jiegou Huaxue(Chin.)(Chin. J. Struct. Chem.)* **2**, 25.
Madhusudhanan, M. C., Balan, H., Werz, D. B. & Sureshan, K. M. (2021). *Angew. Chem. Int. Ed.* **60**, 22797–22803.
Missioui, M., Guerrab, W., Alsubari, A., Mague, J. T. & Ramli, Y. (2022*a*). *IUCrData* **7**, x220621.
Missioui, M., Guerrab, W., Alsubari, A., Mague, J. T. & Ramli, Y. (2022*b*). *Acta Cryst.* E**78**, 855–859.
Missioui, M., Guerrab, W., Mague, J. T. & Ramli, Y. (2020). *Z. Kristallogr. New Cryst. Struct.* **235**, 1429–1430.
Missioui, M., Lgaz, H., Guerrab, W., Lee, H.-S., Warad, I., Mague, J. T., Ali, I. H., <Essassi, El, M. & Ramli, Y. (2022*c*). *J. Mol. Struct.* **1253**, 132132.

Patrick, G. L. (2023). *An introduction to medicinal chemistry*. Oxford University Press.

Petsalakis, E. I., Chrysina, E. D., Tiraidis, C., Hadjiloi, T., Leonidas, D. D., Oikonomakos, N. G., Aich, U., Varghese, B. & Loganathan, D. (2006). *Bioorg. Med. Chem.* **14**, 5316–5324.

Rai, R., Xavier, D., Pathak, S., Fernandez, F. B., Komath, M. & Sureshan, K. M. (2025). *Angew. Chem. Int. Ed.* **64**, e202422593.

Rigaku OD (2026). *CrysAlis PRO*. Rigaku Oxford Diffraction, Yarnton, England.

Sandra, C.-M., Eduardo, C. C., Simon, H.-O., Teresa, R. A., Antonio, N. C., Lijanova, I. V. & Marcos, M.-G. (2012). *Anticancer Agents Med. Chem.* **12**, 611–618.

Sheldrick, G. M. (2015*a*). *Acta Cryst.* A**71**, 3–8.

Sheldrick, G. M. (2015*b*). *Acta Cryst.* C**71**, 3–8.

Spackman, P. R., Turner, M. J., McKinnon, J. J., Wolff, S. K., Grimwood, D. J., Jayatilaka, D. & Spackman, M. A. (2021). *J. Appl. Cryst.* **54**, 1006–1011.

Tan, S. L., Jotani, M. M. & Tiekink, E. R. T. (2019). *Acta Cryst.* E**75**, 308–318.

Zhou, C.-H. & Wang, Y. (2012). *Curr. Med. Chem.* **19**, 239–280.

full crystallographic data

IUCrData (2026). **11**, x261050 [https://doi.org/10.1107/S2414314626010503]

2-Azido-*N*-(*o*-tolyl)acetamide

Abderrazzak El Moutaouakil Ala Allah, Musa A. Said, Vera Lederer, Biprajit Sarkar, Abdulsalam Alsubari, Joel T. Mague and Youssef Ramli

2-Azido-*N*-(2-methylphenyl)acetamide

Crystal data

$C_9H_{10}N_4O$
M_r = 190.21
Triclinic, $P\overline{1}$
a = 4.8642 (6) Å
b = 9.9359 (13) Å
c = 10.4042 (9) Å
α = 70.153 (10)°
β = 87.279 (8)°
γ = 84.833 (10)°
V = 470.97 (10) Å^3
Z = 2
$F(000)$ = 200
D_x = 1.341 Mg m^{-3}
Cu $K\alpha$ radiation, λ = 1.54184 Å
Cell parameters from 1534 reflections
θ = 4.5–72.6°
μ = 0.77 mm^{-1}
T = 250 K
Plank, colourless
0.46 × 0.16 × 0.13 mm

Data collection

SuperNova, Dual, Cu at home/near, Atlas diffractometer
Radiation source: micro-focus sealed X-ray tube, SuperNova (Cu) X-ray Source
Mirror monochromator
Detector resolution: 10.5082 pixels mm^{-1}
ω scans
Absorption correction: gaussian (CrysAlisPro; Rigaku OD, 2026)
T_{min} = 0.474, T_{max} = 1.000
2964 measured reflections
1787 independent reflections
1446 reflections with $I > 2\sigma(I)$
R_{int} = 0.018
θ_{max} = 72.8°, θ_{min} = 4.5°
h = −5→5
k = −11→12
l = −7→12

Refinement

Refinement on F^2
Least-squares matrix: full
$R[F^2 > 2\sigma(F^2)]$ = 0.039
$wR(F^2)$ = 0.116
S = 1.05
1787 reflections
159 parameters
48 restraints
Primary atom site location: dual
Hydrogen site location: mixed
H atoms treated by a mixture of independent and constrained refinement
$w = 1/[\sigma^2(F_o^2) + (0.0606P)^2 + 0.0544P]$ where $P = (F_o^2 + 2F_c^2)/3$
$(\Delta/\sigma)_{max} < 0.001$
$\Delta\rho_{max}$ = 0.22 e Å^{-3}
$\Delta\rho_{min}$ = −0.16 e Å^{-3}

Special details

Geometry. All esds (except the esd in the dihedral angle between two l.s. planes) are estimated using the full covariance matrix. The cell esds are taken into account individually in the estimation of esds in distances, angles and torsion angles; correlations between esds in cell parameters are only used when they are defined by crystal symmetry. An approximate (isotropic) treatment of cell esds is used for estimating esds involving l.s. planes.

Refinement. The crystals contain a disordered azide moiety. The azide consist of N atoms N2-4 (Part 1) and N2A-4A (Part 2) The distances of the disordered groups were restrained to be similar (SADI) and the thermal parameters were also restrained (SIMU, RIGU. The occupancies were allowed to freely refine to sum unity, with a ratio of Part1:part2 of 0.74 (1):0.26 (1).
All hydrogen atoms except H1 were observed in the electron density map before placing and refining using a riding model. Hydrogen atom H1 was refined and the N-H distance restrained to a target value of 0.88 %A (DFIX). The isotropic dispalcement parameters of hydrogen atom H1 was fixed at a value of 1.2 Ueq of the parent nitrogen atom N1.

Fractional atomic coordinates and isotropic or equivalent isotropic displacement parameters (Å²)

	x	*y*	*z*	U_{iso}*/U_{eq}	Occ. (<1)
O1	0.04695 (19)	0.74648 (14)	0.48779 (12)	0.0551 (3)	
N1	0.4802 (2)	0.72303 (14)	0.40158 (12)	0.0400 (3)	
N3	0.0729 (8)	0.9021 (4)	0.6931 (5)	0.0494 (9)	0.740 (4)
C3	0.4099 (3)	0.68309 (16)	0.28864 (14)	0.0374 (3)	
C1	0.2968 (3)	0.75172 (17)	0.49098 (14)	0.0400 (3)	
C4	0.5213 (3)	0.75306 (16)	0.15991 (15)	0.0395 (3)	
C8	0.2337 (3)	0.57458 (17)	0.30866 (16)	0.0458 (4)	
H8	0.163675	0.526827	0.396628	0.055*	
C5	0.4474 (3)	0.71126 (19)	0.05240 (17)	0.0493 (4)	
H5	0.520754	0.756276	−0.035484	0.059*	
C9	0.7116 (3)	0.87048 (18)	0.13746 (16)	0.0475 (4)	
H9A	0.619476	0.946175	0.166719	0.071*	
H9B	0.760659	0.909159	0.041157	0.071*	
H9C	0.877472	0.831851	0.190031	0.071*	
N4	−0.1164 (15)	0.9030 (10)	0.7588 (10)	0.081 (2)	0.740 (4)
C7	0.1620 (3)	0.53715 (19)	0.19932 (19)	0.0548 (4)	
H7	0.040316	0.465146	0.212335	0.066*	
C2	0.4226 (3)	0.7929 (2)	0.60148 (17)	0.0516 (4)	
H2AA	0.417820	0.712307	0.687708	0.062*	0.740 (4)
H2AB	0.616616	0.810274	0.577377	0.062*	0.740 (4)
H2BC	0.603671	0.739849	0.623958	0.062*	0.260 (4)
H2BD	0.452032	0.895441	0.565423	0.062*	0.260 (4)
C6	0.2689 (3)	0.6053 (2)	0.07137 (18)	0.0557 (4)	
H6	0.220633	0.579867	−0.003277	0.067*	
N2	0.2826 (4)	0.9194 (2)	0.6216 (2)	0.0573 (7)	0.740 (4)
N2A	0.2616 (11)	0.7659 (7)	0.7216 (5)	0.0549 (17)	0.260 (4)
N3A	0.065 (2)	0.8486 (12)	0.7275 (15)	0.053 (3)	0.260 (4)
N4A	−0.121 (5)	0.921 (3)	0.740 (3)	0.087 (6)	0.260 (4)
H1	0.651 (4)	0.737 (3)	0.412 (2)	0.104*	

Atomic displacement parameters (Å²)

	U^{11}	U^{22}	U^{33}	U^{12}	U^{13}	U^{23}
O1	0.0242 (5)	0.0869 (9)	0.0647 (7)	−0.0092 (5)	0.0024 (5)	−0.0385 (7)
N1	0.0240 (6)	0.0584 (8)	0.0420 (7)	−0.0063 (5)	−0.0007 (5)	−0.0219 (6)
N3	0.0376 (14)	0.067 (2)	0.057 (2)	−0.0111 (16)	0.0033 (12)	−0.0374 (19)
C3	0.0257 (6)	0.0461 (8)	0.0435 (8)	−0.0003 (5)	−0.0042 (5)	−0.0194 (6)
C1	0.0279 (7)	0.0510 (8)	0.0430 (8)	−0.0059 (6)	0.0001 (5)	−0.0177 (6)

C4	0.0283 (7)	0.0478 (8)	0.0449 (8)	−0.0012 (6)	−0.0014 (5)	−0.0190 (6)
C8	0.0394 (8)	0.0478 (9)	0.0509 (9)	−0.0082 (6)	−0.0004 (6)	−0.0162 (7)
C5	0.0450 (9)	0.0629 (10)	0.0441 (8)	−0.0051 (7)	−0.0003 (6)	−0.0231 (7)
C9	0.0380 (8)	0.0573 (10)	0.0479 (8)	−0.0112 (7)	0.0014 (6)	−0.0168 (7)
N4	0.052 (3)	0.131 (5)	0.083 (3)	−0.024 (2)	0.029 (2)	−0.067 (3)
C7	0.0497 (9)	0.0538 (10)	0.0700 (11)	−0.0138 (7)	−0.0051 (8)	−0.0296 (8)
C2	0.0357 (8)	0.0760 (12)	0.0540 (9)	−0.0089 (7)	0.0023 (6)	−0.0356 (9)
C6	0.0528 (10)	0.0685 (11)	0.0591 (10)	−0.0068 (8)	−0.0072 (8)	−0.0375 (9)
N2	0.0442 (11)	0.0663 (14)	0.0723 (14)	−0.0169 (9)	0.0196 (9)	−0.0370 (11)
N2A	0.051 (3)	0.073 (4)	0.042 (3)	−0.003 (3)	0.002 (2)	−0.021 (3)
N3A	0.045 (4)	0.071 (6)	0.058 (7)	−0.021 (4)	0.006 (4)	−0.037 (5)
N4A	0.070 (10)	0.083 (8)	0.130 (16)	0.008 (6)	−0.010 (8)	−0.068 (9)

Geometric parameters (Å, º)

O1—C1	1.2234 (16)	C9—H9A	0.9700
N1—C3	1.4263 (17)	C9—H9B	0.9700
N1—C1	1.3408 (18)	C9—H9C	0.9700
N1—H1	0.873 (16)	C7—H7	0.9400
N3—N4	1.122 (6)	C7—C6	1.374 (3)
N3—N2	1.223 (4)	C2—H2AA	0.9800
C3—C4	1.392 (2)	C2—H2AB	0.9800
C3—C8	1.392 (2)	C2—H2BC	0.9800
C1—C2	1.515 (2)	C2—H2BD	0.9800
C4—C5	1.391 (2)	C2—N2	1.449 (3)
C4—C9	1.504 (2)	C2—N2A	1.402 (5)
C8—H8	0.9400	C6—H6	0.9400
C8—C7	1.379 (2)	N2A—N3A	1.217 (11)
C5—H5	0.9400	N3A—N4A	1.136 (14)
C5—C6	1.381 (2)		
C3—N1—H1	120.0 (17)	H9A—C9—H9C	109.5
C1—N1—C3	124.46 (11)	H9B—C9—H9C	109.5
C1—N1—H1	115.4 (17)	C8—C7—H7	120.1
N4—N3—N2	171.4 (6)	C6—C7—C8	119.85 (15)
C4—C3—N1	119.13 (12)	C6—C7—H7	120.1
C8—C3—N1	119.80 (13)	C1—C2—H2AA	108.9
C8—C3—C4	121.07 (13)	C1—C2—H2AB	108.9
O1—C1—N1	124.94 (13)	C1—C2—H2BC	108.7
O1—C1—C2	120.59 (13)	C1—C2—H2BD	108.7
N1—C1—C2	114.47 (11)	H2AA—C2—H2AB	107.7
C3—C4—C9	121.38 (13)	H2BC—C2—H2BD	107.6
C5—C4—C3	117.40 (14)	N2—C2—C1	113.38 (15)
C5—C4—C9	121.22 (14)	N2—C2—H2AA	108.9
C3—C8—H8	120.0	N2—C2—H2AB	108.9
C7—C8—C3	119.95 (15)	N2A—C2—C1	114.1 (2)
C7—C8—H8	120.0	N2A—C2—H2BC	108.7
C4—C5—H5	119.1	N2A—C2—H2BD	108.7

C6—C5—C4	121.72 (15)	C5—C6—H6	120.0
C6—C5—H5	119.1	C7—C6—C5	119.99 (15)
C4—C9—H9A	109.5	C7—C6—H6	120.0
C4—C9—H9B	109.5	N3—N2—C2	116.9 (2)
C4—C9—H9C	109.5	N3A—N2A—C2	120.0 (7)
H9A—C9—H9B	109.5	N4A—N3A—N2A	176 (2)
O1—C1—C2—N2	−47.3 (2)	C1—N1—C3—C4	131.37 (16)
O1—C1—C2—N2A	24.8 (4)	C1—N1—C3—C8	−49.2 (2)
N1—C3—C4—C5	−179.88 (13)	C1—C2—N2—N3	81.8 (4)
N1—C3—C4—C9	−0.6 (2)	C1—C2—N2A—N3A	−79.6 (10)
N1—C3—C8—C7	179.04 (14)	C4—C3—C8—C7	−1.5 (2)
N1—C1—C2—N2	132.74 (16)	C4—C5—C6—C7	−0.7 (3)
N1—C1—C2—N2A	−155.1 (3)	C8—C3—C4—C5	0.6 (2)
C3—N1—C1—O1	0.5 (3)	C8—C3—C4—C9	179.96 (14)
C3—N1—C1—C2	−179.52 (14)	C8—C7—C6—C5	−0.1 (3)
C3—C4—C5—C6	0.5 (2)	C9—C4—C5—C6	−178.84 (15)
C3—C8—C7—C6	1.2 (3)		

Hydrogen-bond geometry (Å, º)

*Cg*1 is the centroid of the C3–C8 benzene ring.

D—H···*A*	*D*—H	H···*A*	*D*···*A*	*D*—H···*A*
N1—H1···O1^{i}	0.87 (2)	2.14 (2)	2.9918 (15)	166 (2)
C2—H2*AB*···O1^{i}	0.98	2.37	3.2576 (19)	150
C9—H9*C*···Cg1^{i}	0.97	2.81	3.5817 (18)	137

Symmetry code: (i) *x*+1, *y*, *z*.